

# Photon-correlation velocimetry of polystyrene solutions in extensional flow fields

K. Gardner and E. R. Pike

Royal Signals and Radar Establishment, St. Andrews Road, Malvern, Worcestershire

and M. J. Miles, A. Keller and K. Tanaka

H. H. Wills Physics Laboratory, University of Bristol, Royal Fort, Tyndall Avenue, Bristol  
(Received 21 December 1981)

A cross slot device has been used to produce elongational flow fields in dilute solutions of narrow fractions of high molecular weight ( $M_w$  between  $2.8 \times 10^6$  and  $2 \times 10^7$ ) atactic polystyrene. Strain-rates obtainable were sufficient to extend individual molecules. Photon-correlation microvelocimetry has been used to measure velocity profiles in a channel of the cross slot as a function of distance from the centre of the cross, polymer concentration and flow rate. It has been found that in solutions of concentration about or greater than  $c^*$  and at flow rates sufficient to extend the polymer molecules a minimum in velocity is observed at the centre of the channel. This minimum sets in at flow rates around that at which extension of the polymer molecules is first observed through birefringence observations, but the depth of the minimum decreases rapidly with decreasing polymer concentration below  $c^*$ . The velocity profile evolves into the usual parabolic profile away from the region of elongational flow. At higher strain rates a birefringence in the solution near the channel walls was also observed and preliminary measurements indicate that two symmetrical minima or shoulders in the velocity profile may be associated with this observation.

**Keywords** Photon-correlation velocimetry; elongational flow birefringence; polystyrene solutions; hydrodynamics; adsorbition

## INTRODUCTION

In recent years, there has been increasing interest in the behaviour of polymer molecules in extensional flow fields. The earlier experimental work was concerned with orienting molecules in concentrated solutions using the 4-roll mill<sup>1</sup> or the opposed jets<sup>2</sup> to produce the necessary extensional flowfields. More recently the behaviour of isolated molecules in dilute solution has been studied. The concentrations used must be less than the concentration,  $c^*$ , at which the radii of gyration of the molecules just overlap. At such polymer concentrations and using the opposed jets of cross slot<sup>3,4</sup> the predicted critical strain rate,  $\dot{\epsilon}_c$ <sup>5,6</sup>, at which the molecule goes from an almost unperturbed random-coil state to being almost completely extended in the so-called coil-stretch transition<sup>7</sup> has been observed.

To recapitulate, the experimental effect itself is illustrated by *Figure 1* for the case of the cross-slots (*Figure 2*). Here at a critical strain rate ( $\dot{\epsilon}_c$ ) a birefringent line appears along the exit channels (*Figure 1*). This line itself is confined to the plane (line in edge-on view) along the exit axis of the cross slot. It is sharpest within the cross-over region of the two arms of the channel but persists into and gradually fades out within the outgoing channels. The localization of this birefringence to the central region of cross-gap and exit channel has previously been recognized as being due to the maximum residence time of the fluid elements along flow lines passing through the

stagnation region (the geometric centre point of the flow system as seen in projection). This circumstance has permitted the use of the cross slot in place of the first adopted jets system, because the effect of simple shear at the additional walls forming the inlet channels can in first approximation be ignored in the central region where the



*Figure 1* Basic effect: A sharply defined birefringent line appearing along the exit axis (horizontal) in a cross-slot device as in *Figure 2* at a critical strain rate ( $\dot{\epsilon}_c$ ). Crossed polaroids at  $45^\circ$  to the channels. The channel walls are marked with a dotted white line for better visibility on the print. Irregular bright regions outside the channels are due to faults (scratches, excess glue etc.) within or on the glass cubes used for the construction and are thus to be ignored

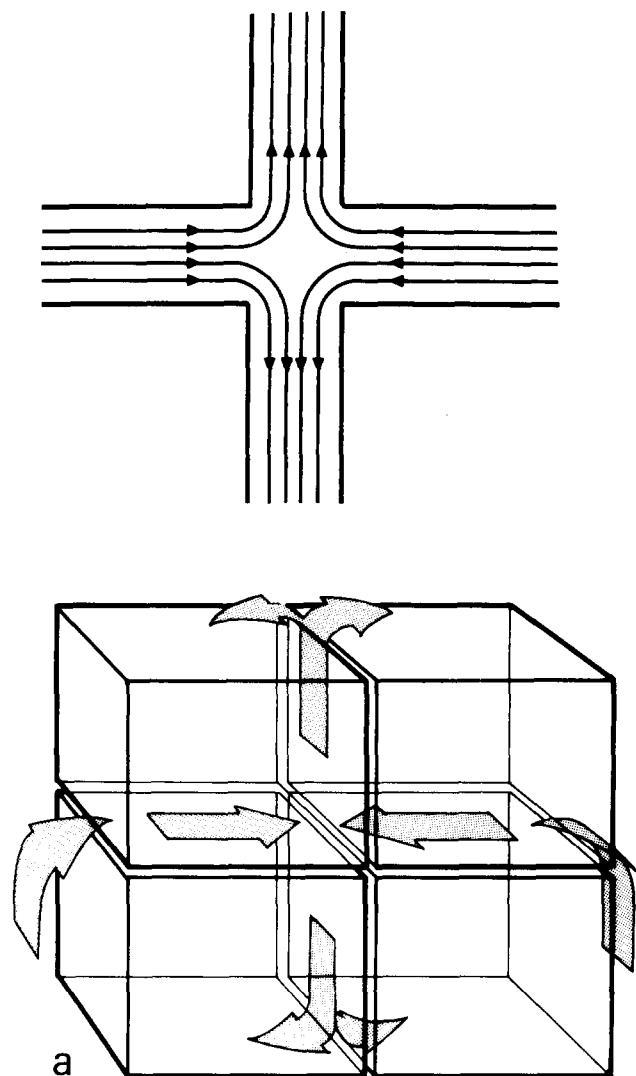


Figure 2(a) Cross-slot device used to produce a planar elongational flow-field

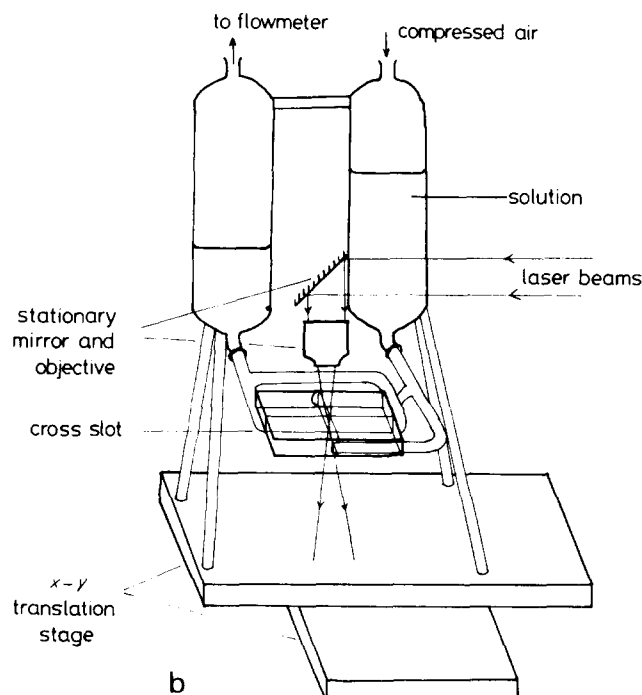


Figure 2(b) Arrangement of cross-slot, reservoirs and translation stage

effects under observation take place. (In brief the flow in the relevant central zone of the channel intersection can in first approximation be regarded as purely elongational).

The relaxation time,  $\tau_{c \rightarrow s}$ , associated with this stretching transition can be found from the relationship:  $\dot{\epsilon}_c \tau_{c \rightarrow s} = 1$ , and  $\tau_{c \rightarrow s}$  has been shown experimentally<sup>3</sup> to correspond to the non-free-draining relaxation time<sup>8</sup>, which depends on the random-coil dimensions. The effect of changes in these dimensions could thus be followed using this technique and a simple power law relating  $\tau_{c \rightarrow s}$  to molecular weight was established.

The aforementioned information is all derivable from  $\dot{\epsilon}_c$  itself obtainable through observing the sudden onset of the central birefringent line at the channel cross-over region. As seen in *Figure 1*, this line continues within the exit channel. Its decay along this channel gives a measure of the retraction time of the stretched out molecule, hence the corresponding relaxation time  $\tau_{s \rightarrow c}$ . This is of special interest, particularly as it has been predicted that the free retraction of the stretched out molecule to the coil state will be much slower, hence  $\tau_{s \rightarrow c}$  is longer than the corresponding  $\tau_{c \rightarrow s}$  which pertains to the initial extension of the coil. Indeed such a hysteresis in relaxation times has been directly verified previously by cross-slot experiments of the present kind<sup>4</sup> and a value was assigned to  $\tau_{s \rightarrow c}$  (in fact two values, as the retraction was found to be a two stage process). This was done on the assumption that the velocity gradient along the centre line *within* the exit channel is zero, i.e. no extensional force will be acting on the chain once it enters the channel, which will thus obey the law of free recoil.

The past works referred to relied on strain rate values determined from macroscopic flow velocity measurements. While there could be never any doubt that the trends observed were genuine the exact numerical values of the relaxation times will depend on the reliability of the knowledge of the strain rate which pertains locally in the restricted region of the flow field where the molecule extends or retracts. The extension of the molecule comes about through frictional coupling of the extensional flow field with the molecule. Thus extending the molecule, or maintaining this extension against the entropic retractive force of the molecule, involves the dissipation of energy from the flow field. This may result in a local decrease in the flow velocity in the restricted central region where chain extension or subsequent retraction occurs. In refs. 3 and 4, while recognizing the possibility of the flow modifying effect of the presence of stretched molecules, such an effect was considered negligible for the dilute solutions used. Since then Scrivener *et al.*<sup>9</sup> have observed such an effect in the form of a central minimum in the velocity profiles across the exit channel of a cross-slot like ours (they were first to use cross-slots) for polyethylene oxide solutions. The concentrations involved, where such effects were seen were much higher than in any previous experiments, and certainly above  $c^*$ , in materials which in addition had broad molecular weight distributions. Also no indication was given as to whether a critical strain rate has been observed or how the observed central minimum in velocity changed with strain rate in the region which potentially could have been close to the critical value. Nevertheless these observations in ref. 9 coupled with the reservations made by ourselves in refs. 3 and 4, necessitated the examination of the problem of the potential effect which the extension of the molecules may

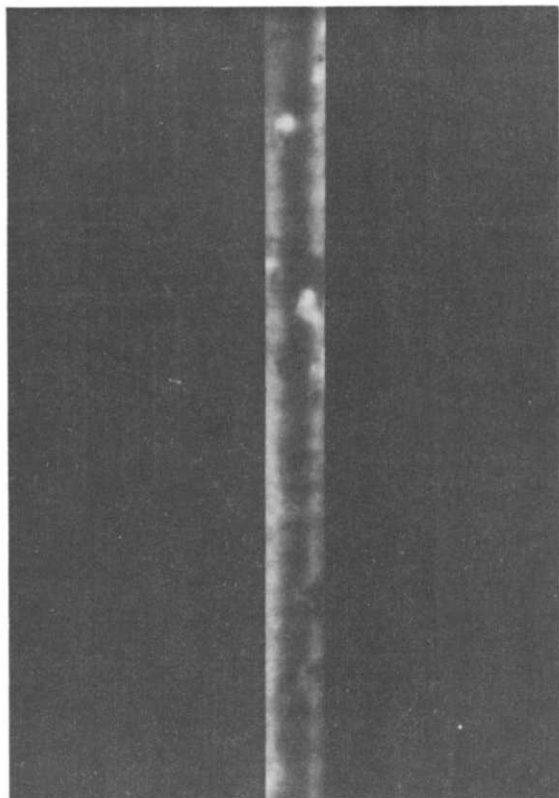


Figure 3 Part of cross-slot channel showing birefringence in solution near the walls at high flow rates (in this case entry channel)

have on the flow field. This was undertaken in the present work, firstly in order to reassure ourselves that the values of  $\tau_{c \rightarrow s}$  and  $\tau_{s \rightarrow c}$  and their molecular weight dependence claimed in refs. 3 and 4 can be quantitatively upheld and secondly because of the intrinsic interest of the subject, namely possible flow modification by stretched molecules as such. As will be seen, in the light of these studies the earlier conclusions in refs. 3 and 4 remain valid, nevertheless, flow modifications were registered in a striking way at higher concentrations.

The work in question acquired a further dimension through the observation of a new effect made since the publication of refs. 3 and 4. Namely, at sufficiently high flow rates a birefringent zone could appear along the walls of the channels, both exit and entry. This appeared with approximately constant intensity along the entire length of the channels (see Figure 3) irrespective of the presence or absence of the central birefringent line, which in the case of the exit channel could appear simultaneously with the wall effect. As a secondary aim of this work the local velocity was also explored in cases where such a wall effect appeared with appropriate emphasis on regions of the flow field near the walls.

Photon-correlation velocimetry<sup>10</sup> was considered the most appropriate technique for the measurement of velocity profiles in the cross slot as it is a non-invasive method which can provide the required resolution across the channel ( $\sim 5 \mu\text{m}$ ), and is suitable for the range of velocities under investigation. Some preliminary results of the work have already been reported<sup>11</sup>. The present paper now provides further information. Regrettably, owing to external constraints the examination could still not be made as complete as the intrinsic interest of the subject may require.

## EXPERIMENTAL

A cross slot (Figure 2a) of glass with 20 mm channels of cross section  $250 \mu\text{m} \times 4 \text{mm}$  was constructed, the channel walls having been polished optically flat to reduce light scattering at this interface. The possibility of turbulence would have been reduced if the corners at the centre of the cross had been rounded. This, however, proved to be practically difficult on this scale, though clearly not impossible if shown to be important; there does not appear to have been a turbulence problem in this respect, and no separation of the flow at the edges was observed.

Solutions of narrow fractions of atactic polystyrene (PS) of  $\bar{M}_w = 2.8 \times 10^6$  ( $\bar{M}_w/\bar{M}_n = 1.3$ ),  $\bar{M}_w = 7.2 \times 10^6$  ( $\bar{M}_w/\bar{M}_n = 1.3$ ) and  $\bar{M}_w = 2 \times 10^7$  ( $\bar{M}_w/\bar{M}_n = 1.3$ ) were dissolved in either *o*-xylene or a dekaline/tetralin (32.9:67.1) mixture at concentrations between 0.001% (w/v) and 0.35%. The mixed solvents were used to match the refractive index of the solution to that of the glass, in order to reduce scatter of the laser beams at the solution/glass interface during measurements to the channel wall. The solution was forced through the cross slot from one reservoir to the other (Figure 2b) by increased air pressure above the solution in the first reservoir, producing the flow directions indicated in Figure 2a. The flow rate was determined by measuring the displacement of air from the second reservoir using a capillary flow manometer.

The optical system used is shown in Figure 4. The argon-ion laser ( $\lambda = 488 \text{nm}$ ) was run at about 20 mW. The two beams from the beam splitter were crossed in the cell at their waists using a  $\times 25$  Leitz microscope objective. The beam waist was about  $5 \mu\text{m}$  with a fringe spacing of  $1.68 \mu\text{m}$ , aligned to measure the velocity component along the channel. It was possible to measure velocities to within about  $10 \mu\text{m}$  of the channel walls without the diffraction spread of the beams impinging on the walls (at a grazing angle) and the resulting scattered light degrading the signal to an unacceptable degree. The light from the scattering volume was received through an aperture, at an angle of about  $110^\circ$ , by a long focal length (50 mm) microscope objective, and imaged on a  $100 \mu\text{m}$  diameter pinhole, which, in turn, was viewed by the standard boresighting optics of a Malvern photon detector, the signals from which were processed by a 50 ns Malvern Correlator. The resultant correlation functions were plotted out on an HP 9830 and also stored on paper tape for later analysis.

The cross slot cell (and reservoirs) were mounted on an X-Y translation stage with stepper-motor drive. This

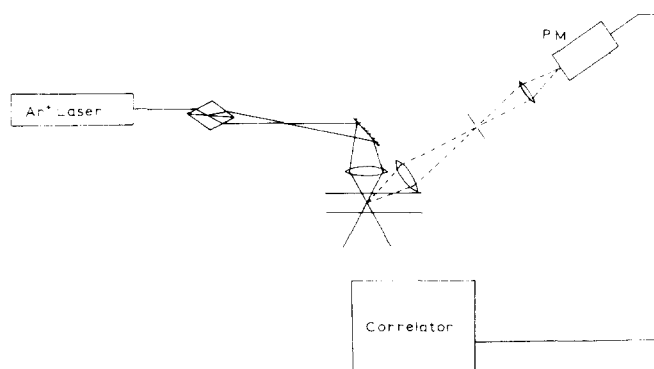


Figure 4 Optical arrangement

allowed the cell to be moved with respect to the crossed laser beams with a minimum step of 1  $\mu\text{m}$ . Measurements were made at 15  $\mu\text{m}$  intervals, except in the case of the velocity measurements under wall-birefringence conditions when the intervals were 5  $\mu\text{m}$ .

Seeding of the solutions with  $\text{TiO}_2$  particles (<2  $\mu\text{m}$  diameter) was necessary in the case of dilute solutions. At an intermediate region of concentration, where a weak signal from the polymer molecules alone could still be easily detected, a comparison of the profiles with and without seeding could be made in order to test the reliability of the profiles obtained with seeding.

RESULTS AND DISCUSSION

A typical correlation function resulting from measurements on a 0.35% solution of a PS ( $\bar{M}_w = 7.2 \times 10^6$ ) in *o*-xylene flowing through the slot device is shown in Figure 5. Data reduction was complicated by the presence, on the same timescale as the signal, of an internal mode scattering of the polystyrene molecule, which gave an exponential correlation function

of decay time approximately 30  $\mu\text{s}$ . A 'six-parameter Gaussian' fit, however, still gave accurate frequency values (Figure 5).

In the case of correlation functions from dilute solution with  $\text{TiO}_2$  seeding, the internal molecular modes are less prominent, but Brownian motion of the scattering particles is apparent. Although a decay resulting from the finite size of the probe must be present in regions of high transverse velocity gradient, it was not possible to ascribe the observed decay to this cause.

Velocity profiles for concentrated solutions at several positions along a channel

Flow velocities, determined from the correlation functions, were measured at 15  $\mu\text{m}$  intervals across the channel at several positions down the channel from the centre of the cross and in both extensional, i.e. away from the cross, and normal or compressional, i.e. towards the centre of the cross, flow directions for a 0.35% solution of PS ( $\bar{M}_w = 7.2 \times 10^6$ ). This is regarded as a concentrated solution as  $c^*$  for this polymer is about 0.08%. This higher concentration was used in the first experiments in order to obtain a positive effect.

The velocity profiles at several positions along the channel for three different total flow rates are shown in Figure 6. The most striking feature is the central minimum in the velocity for the flow in the extensional direction (solid line), i.e. away from the centre of the cross. The minimum is deepest nearest the centre of the cross, and the profiles evolve along the channel into the normal parabolic velocity profile. For the same total flow rate, this parabolic profile closely resembles the profiles for flow in the normal (or compressional) direction (broken line).

The area under the velocity profiles, for a given total flow rate, increases with increasing distance along the channel. This is the case for both the normal and extensional flow directions, but is greater in the latter case. If the solution is assumed to be incompressible, then this suggests that the velocity profile across the depth of the channel (i.e. in a direction perpendicular to the page) changes from being flat near the channel entrance to a steeper, most likely parabolic, profile further down the channel.

It can be seen in Figure 6 that the central minimum in

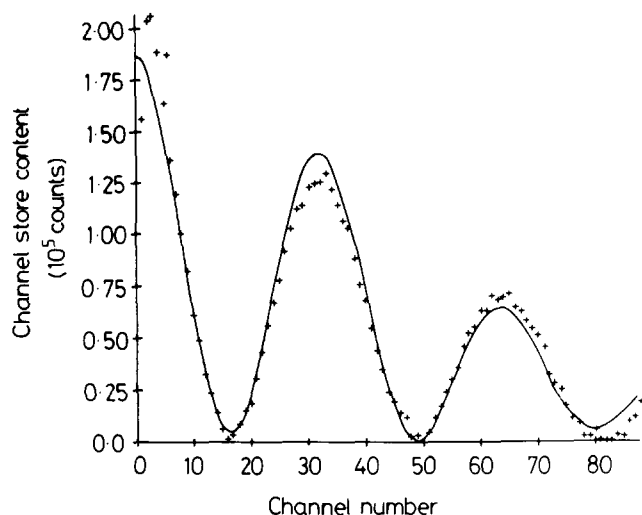


Figure 5 Typical correlation function from 0.35% solution of PS ( $\bar{M}_w = 7.2 \times 10^6$ ) in *o*-xylene. + Are data points and the solid line is a fitted curve

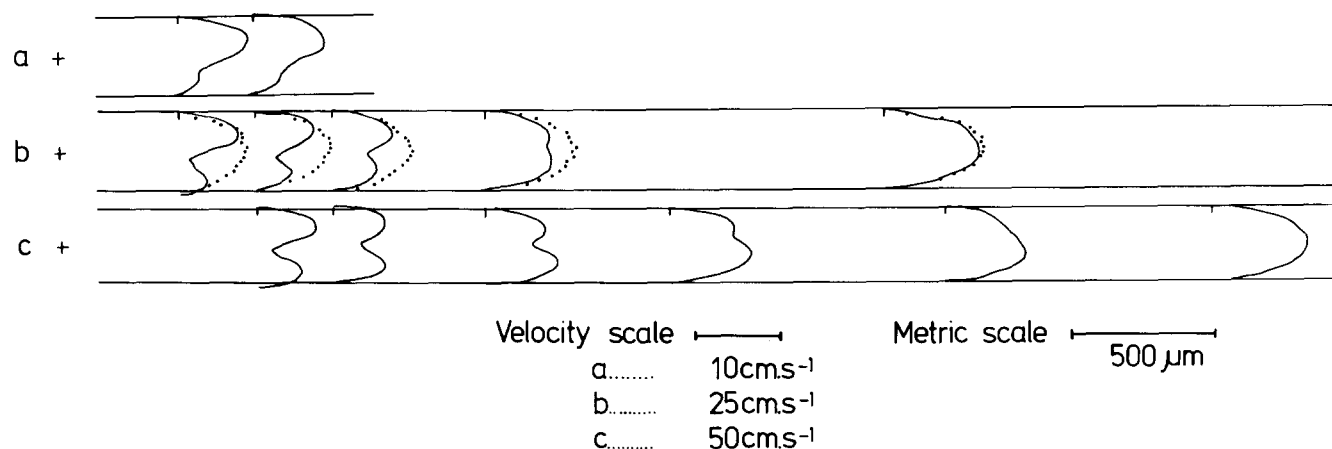


Figure 6 Velocity profiles at several positions along the channel for the three flow rates indicated by the scale bar. Flow in the extensional direction, i.e. away from the centre of the cross (—); flow in the compressional direction, i.e. towards the centre of the cross, (.....); (+) represents the centre of the cross slot

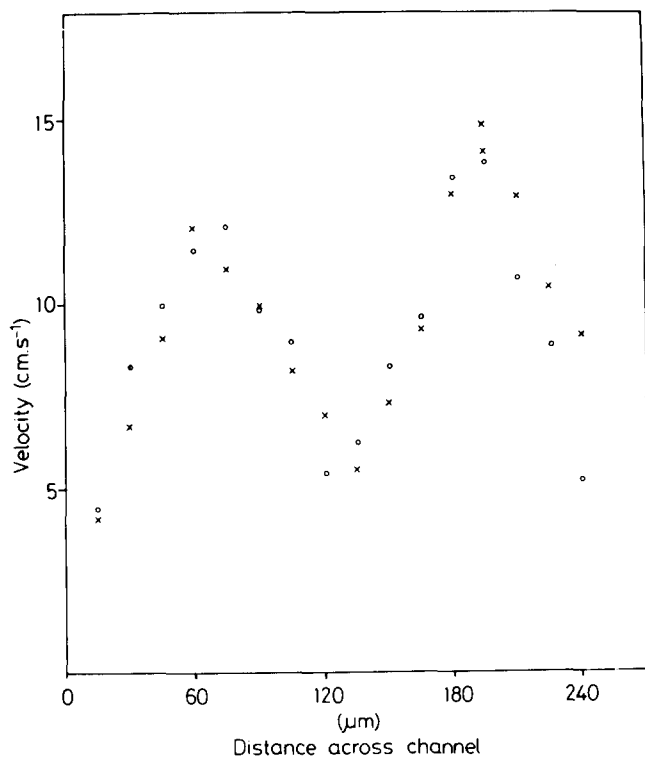


Figure 7 Comparison of the velocity profile obtained at 1.5 mm down the channel from scattering by polymer molecules without added seed (O) and of the profile obtained from scattering predominantly by added  $\text{TiO}_2$  seed (X). The solution was 0.35% PS ( $M_w = 2 \times 10^7$ ) in tetralin/decalin

the profile persists further down at the higher flow rates. The persistence of the minimum down the channel from the centre cross may reflect a momentum defect resulting from the local decrease in velocity in the centre of the cross due to extension of the molecules. This would be similar to the minimum in the velocity profile found downstream from a stationary sheet placed in a flowing fluid. Another possibility is that the minimum is in some way a result of the higher viscosity associated with extended molecules, the effect decaying as the molecules retract further along the channel. It is, however, difficult to make any quantitative analysis of the profile evolution, and, in particular, the disappearance of the central minimum, as the profiles are in many cases very asymmetric about the central line. It should be mentioned that the profiles measured are those for a planar section about halfway through the depth of the channel, while the flow may be 3-dimensional as a result of imperfections in the cell construction. Alternatively, such asymmetries in the flow field may be inherent in a cell of this size and geometry due to fluidic-type instabilities.

#### Concentration dependence of the central minimum

These measurements were made on solutions of PS of  $M_w = 2 \times 10^7$  in a tetralin/decalin mixture above the theta temperature. The concentrations were less than or equal to  $c^*$ , which is about 0.035% (w/v) for this polymer. At low concentrations it was necessary to add  $\text{TiO}_2$  seed to improve the signal. However, at a polymer concentration of 0.04%, it was possible to obtain a velocity profile both with and without seed. Figure 7 shows this comparison. The profiles obtained are, within experimental error, the same, and so it has been assumed that the added scattering

particles do not significantly perturb the flow field at lower polymer concentrations where such comparisons were not possible.

The results illustrating the dependence of the velocity profile (at a fixed distance of 1.5 mm down the channel) on the polymer concentration are shown in Figure 8. The polymer concentration range is from 0% (pure solvent + seed) to 0.04%, i.e. slightly greater than  $c^*$ . It can be seen that there is a strong dependence of the depth of the central minimum on the concentration in the region of  $c^*$ . The depth of the minimum does not change greatly for concentrations of four times  $c^*$  shown in Figure 6. This suggests that the minimum may be the result of some intermolecular interaction that can occur at concentrations around  $c^*$  or greater. At concentrations below  $c^*$  the depth of the velocity minimum decreases rapidly with concentration to an extent such that it may be possible to neglect its effect on the flowfield.

#### Strain-rate dependence of the central minimum

The strain-rate or flow-rate dependence of the velocity profile (at a fixed distance of 1.5 mm along the channel) is illustrated in Figure 9. Profiles are shown for a range of flow rates covering the critical value of flow ( $\sim 7.7 \text{ ml min}^{-1}$ ) corresponding to  $\dot{\epsilon}_c$  at which the birefringent line is first observed. It can be seen that it is above this critical value of flow that the central minimum is first clearly seen, the depth of the minimum increasing as the intensity of the associated birefringent line initially increases with flow rate. This demonstrates that the minimum in the flow profile is associated with the extension of molecules at  $\dot{\epsilon}_c$  in the centre of the cross. This result indicates that at the initial onset of molecular extension when only a very small fraction, the longer molecules, of the polymer has been extended, the effect on the flow field is also small. The measurement of the critical strain rate,  $\dot{\epsilon}_c$ , has in the past<sup>3</sup> been performed by establishing the flow rate at which the onset of birefringence resulting from molecular extension could first be observed, i.e. before the flow field would have been significantly modified. Any modification would again be reduced by the use of dilute solutions, as was seen in the previous section. The conclusions of the previous work remain valid under the conditions of measurement pertaining.

The assumption of constant velocity profile along the channel made in order to estimate the relaxation times,  $\tau_{s \rightarrow c}$ , associated with the retraction of the stretched molecule<sup>4</sup>, is less satisfactory as flow rates above the critical value were used. The estimate of  $\tau_{s \rightarrow c}$  will be a good first order approximation, and, will, in fact have been an underestimate. This means that the difference between  $\tau_{c \rightarrow s}$  and  $\tau_{s \rightarrow c}$  is greater, and therefore in closer agreement with theoretical predictions<sup>7</sup>.

#### Velocity profile under wall-birefringence conditions

During the course of birefringence observation in the cross-slot it was noted that at sufficiently high flow rates, and with the polars crossed and oriented at  $45^\circ$  with respect to the channels, a birefringent region extended some  $60 \mu\text{m}$  from the channel walls into the flowing solution. Figure 3 shows this effect. The birefringence was of uniform intensity along the entire length of the channel, and if the solution was allowed to flow freely from the ends of the exit channels into more solution surrounding the cross-slot, then the birefringence was observed to persist

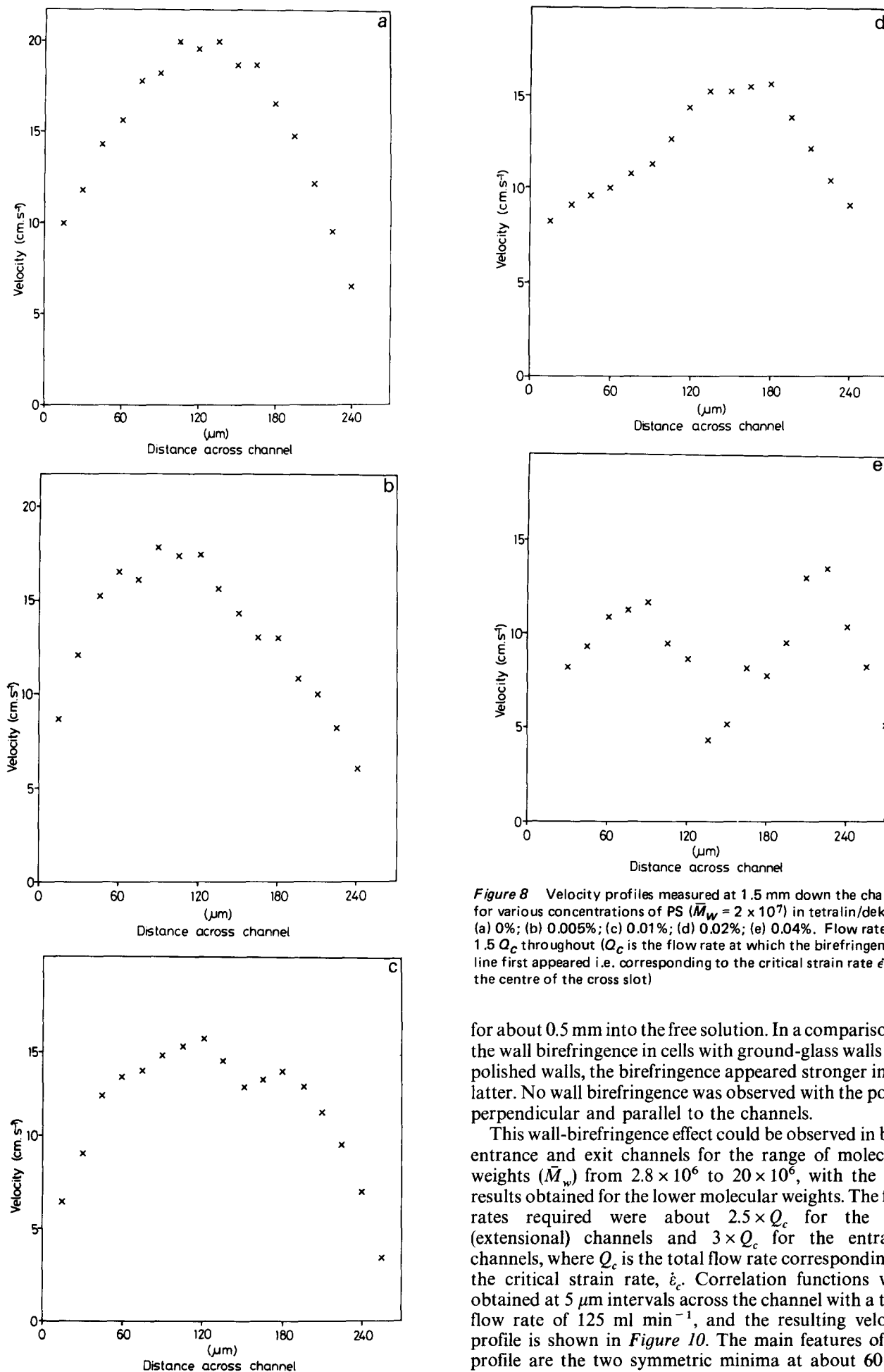


Figure 8 Velocity profiles measured at 1.5 mm down the channel for various concentrations of PS ( $\bar{M}_w = 2 \times 10^7$ ) in tetralin/dekalin: (a) 0%; (b) 0.005%; (c) 0.01%; (d) 0.02%; (e) 0.04%. Flow rate:  $1.5 Q_c$  throughout ( $Q_c$  is the flow rate at which the birefringent line first appeared i.e. corresponding to the critical strain rate  $\dot{\epsilon}_c$  in the centre of the cross slot)

for about 0.5 mm into the free solution. In a comparison of the wall birefringence in cells with ground-glass walls and polished walls, the birefringence appeared stronger in the latter. No wall birefringence was observed with the polars perpendicular and parallel to the channels.

This wall-birefringence effect could be observed in both entrance and exit channels for the range of molecular weights ( $\bar{M}_w$ ) from  $2.8 \times 10^6$  to  $20 \times 10^6$ , with the best results obtained for the lower molecular weights. The flow rates required were about  $2.5 \times Q_c$  for the exit (extensional) channels and  $3 \times Q_c$  for the entrance channels, where  $Q_c$  is the total flow rate corresponding to the critical strain rate,  $\dot{\epsilon}_c$ . Correlation functions were obtained at  $5 \mu\text{m}$  intervals across the channel with a total flow rate of  $125 \text{ ml min}^{-1}$ , and the resulting velocity profile is shown in Figure 10. The main features of the profile are the two symmetric minima at about  $60 \mu\text{m}$

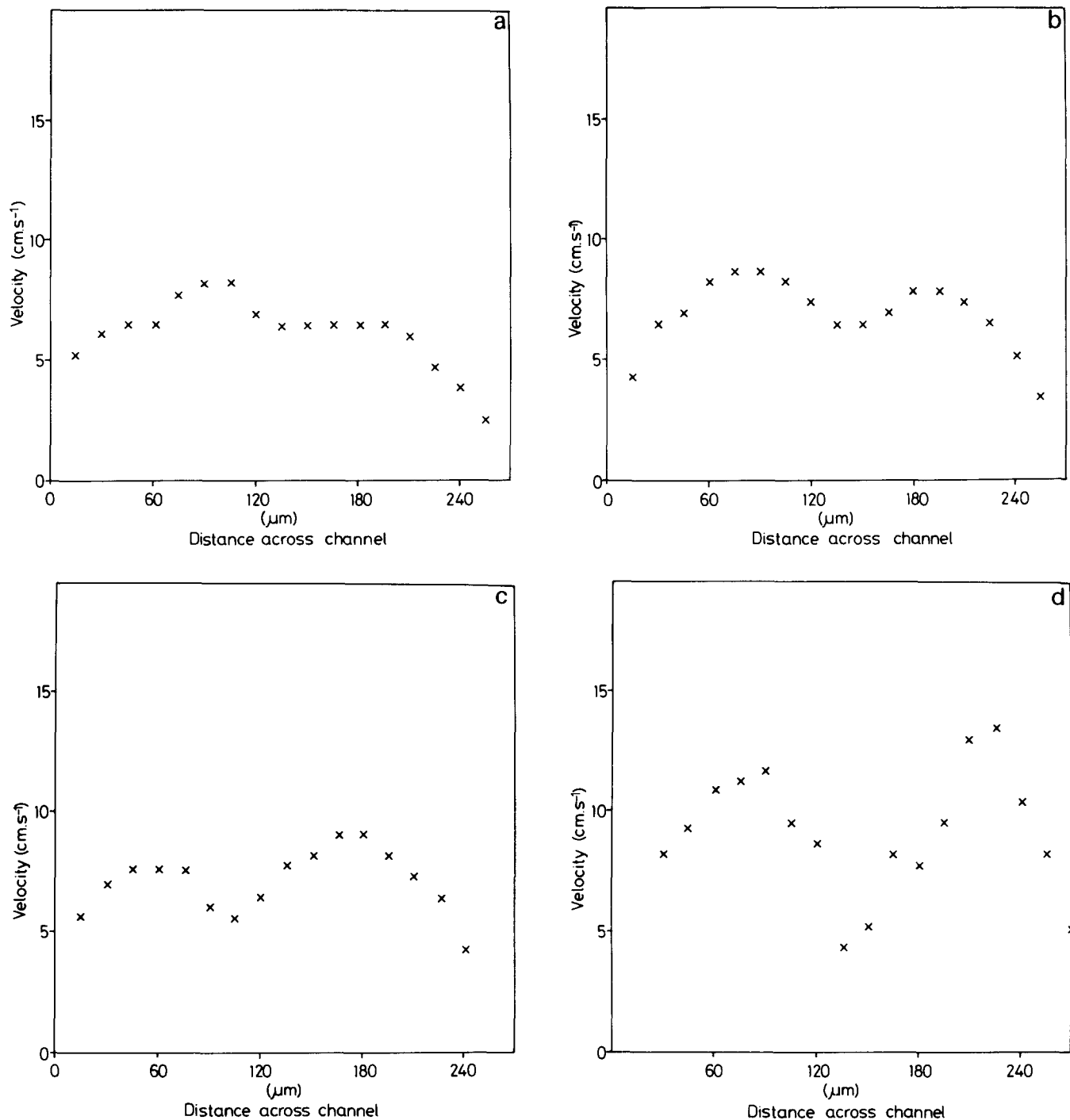


Figure 9 Velocity profiles measured at 1.5 mm down the channel for various overall flow rates: (a)  $0.8 Q_C$ ; (b)  $Q_C$ ; (c)  $1.3 Q_C$ ; (d)  $1.5 Q_C$ . Molecular weight was  $2 \times 10^7$  and concentration 0.04%

from the walls. Measurement of the profile was repeated several times at two positions along the channel (1.5 mm and 2.2 mm from the cross) over a period of several hours and these minima, or, in some cases, shoulders were always found.

If these minima are associated with the wall birefringence and are therefore assumed to represent the steady state, then they cannot be explained by pure hydrodynamic arguments alone, as the regions of negative shear would require a negative value for viscosity.

Frank<sup>12</sup> has suggested that the minima may be a result of an entanglement layer of polymer attached to the channel wall. Preliminary calculations indicate that such entanglements could produce concavities in the velocity

profile, depending on the profile and density assumed for this entanglement layer. Observations of adsorption to a glass surface of an entangled polymer layer under flow conditions have been reported previously<sup>13</sup>. The intensity of the wall birefringence was less than the intensity of the localized central line, which is that associated with extended molecules, but it was of the same order and, therefore, greater than would be expected in the usual transverse-gradient flow birefringence systems such as the Couette.

## CONCLUSIONS

The measurements reported clearly demonstrate an

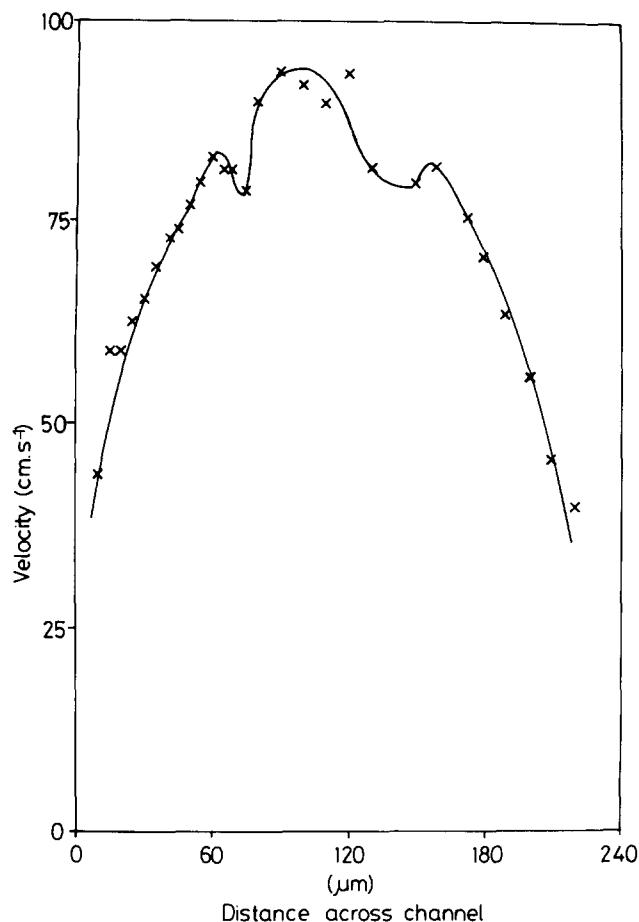


Figure 10 Velocity profile obtained under conditions at which wall birefringence could be observed. The solution was 0.1% PS ( $\bar{M}_w = 2.8 \times 10^6$ ) in tetralin/decalin and the flow rate was 124 ml/min. This profile was measured at 1.5 mm from the centre of the cross

interaction between molecular extension and flow field. At this stage these can form only a preliminary survey of what can now be seen as a new and complex field of study. However, the conditions for which perturbation of the flowfield by molecular extension is small have been mapped out. These conditions comprise the use of dilute solutions ( $c < c^*$ , and preferably as dilute as detection techniques allow), and flow rates not much in excess of that required by attainment of  $\dot{\epsilon}_c$  (as it was found that the initial onset of birefringence had little effect on the flow field). These were the conditions used in previous measurements<sup>3</sup> of  $\dot{\epsilon}_c$ , and so the validity of our previous

approach leading to the determination of  $\tau_{c \rightarrow s}$  and  $\tau_{s \rightarrow c}$  is safeguarded.

The measured velocity profiles under conditions where wall-birefringence could be observed form a preliminary investigation into what appears to be a previously unreported observation. If the hypothesis of an entanglement layer attached to the wall proves to be correct then the nature of the surface involved in this polymer adsorption would be of utmost importance which in turn would be of utmost importance also for polymer adsorption studies in general. It would imply amongst others that the nature of the surfaces involved should have a significant effect for the study of chain dynamics and for the hydrodynamics of polymer solutions in general. Further investigations would involve consideration of the mechanism by which partially extended molecules could become attached to various surfaces.

As a still wider generality the results presented raise new issues in the field of non-Newtonian hydrodynamics, a rigorous analysis of which may be complex or require the development of a new approach.

#### ACKNOWLEDGEMENT

M.J.M. and K.T. wish to thank the Science and Engineering Research Council for financial support.

#### REFERENCES

- 1 Pope, D. P. and Keller, A. *Colloid Polym. Sci.* 1977, **255**, 633
- 2 Mackley, M. R. and Keller, A. *Phil. Trans. Roy. Soc. (London)* 1975, **278**, 29
- 3 Farrell, C. J., Keller, A., Miles, M. J. and Pope, D. P. *Polymer* 1980, **21**, 1292
- 4 Miles, M. J. and Keller, A. *Polymer* 1980, **21**, 1295
- 5 Peterlin, A. *J. Polym. Sci. B* 1966, **4**, 287
- 6 Hlavacek, B. and Seyer, F. A. *Kolloid Z.Z. Polymere* 1971, **243**, 32
- 7 De Genneš, P. G. J. *J. Chem. Phys.* 1974, **60**, 5030
- 8 Zimm, B. H. J. *J. Chem. Phys.* 1956, **24**, 269
- 9 Lyazid, A., Scrivener, O., Teitgen, R. in 'Rheology' (Eds. G. Astarita, G. Marrucci and L. Nicolais), Plenum Pub. Corp., New York, v. 2, p. 141 (1980)
- 10 See for example 'Photon Correlation Spectroscopy and Velocimetry' (Eds. H. Z. Cummins and E. R. Pike), Plenum Press, New York, 1977
- 11 Gardner, K., Miles, M. J., Keller, A. and Pike, E. R. in Proc. 4th Int. Conf. on Photon Correlation Techniques in Fluid Mechanics (Eds. W. Mayo and A. E. Smart), Stanford Univ., 1980
- 12 Frank, F. C. private communication
- 13 Hand, J. H. and Williams, M. C. *Chem. Eng. Sci.* 1973, **28**, 63